JOC*Article*

Nitrenes, Diradicals, and Ylides. Ring Expansion and Ring Opening in 2-Quinazolylnitrenes

David Kvaskoff, Pawel Bednarek, Lisa George, Kerstin Waich, and Curt Wentrup*

Chemistry Building, School of Molecular and Microbial Sciences, The University of Queensland, Brisbane, Queensland 4072, Australia

wentrup@uq.edu.au

Received December 12, 2005

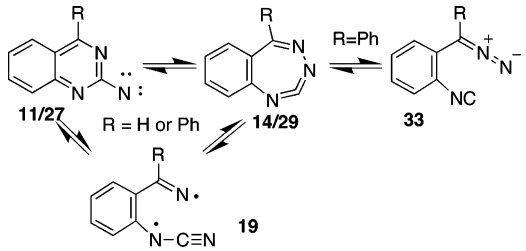

Tetrazolo[1,5-*a*]quinazoline (**9**) is converted to 2-azidoquinazoline (**10**) on sublimation at 200 °C and above, and the azide−tetrazole equilibrium is governed by entropy. 2-Quinazolylnitrenes **11** and **27** and/or their ring expansion products **14** and **29** can undergo type I (ylidic) and type II (diradicaloid) ring opening. Argon matrix photolysis of **9**/**10** affords 2-quinazolylnitrene (**11**), which has been characterized by ESR, UV, and IR spectroscopy. A minor amount of a second nitrene, formed by rearrangement or ring opening, is also observed. A diradical (**19**) is formed rapidly by type II ring opening and characterized by ESR spectroscopy; it decays thermally at 15 K with a half-life of ca. 47 min, in agreement with its calculated facile intersystem crossing (**19T** → **19OSS**) followed by facile cyclization/rearrangement to 1-cyanoindazole (**21**) (calculated activation barrier 1−2 kcal/mol) and *N*-cyanoanthranilonitrile (**22**). **21** and **22** are the isolated end products of photolysis. **21** is also the end product of flash vacuum thermolysis. An excellent linear correlation between the zero-field splitting parameter D (cm^{-1}) and the spin density ρ on the nitrene N calculated at the B3LYP/EPRIII level is reported ($R^2 = 0.993$ for over 100 nitrenes). Matrix photolysis of 3-phenyltetrazolo[1,5-*a*]quinazoline (**25**) affords the benzotriazacycloheptatetraene **29**, which can be photochemically interconverted with the type I ring opening product 2-isocyano-α-diazo-α-phenyltoluene (**33**) as determined by IR and UV spectroscopy. The corresponding carbene **37**, obtained by photolysis of **33**, was detected by matrix ESR spectroscopy.

Introduction

The rearrangements of aryl- and heteroarylnitrenes have been the subject of intense interest for several years.[1] Three major types of reaction have been identified: ring expansion to seven-membered ring cumulenes (e.g., **3** or **5**), ring opening to ylides, ketenimines, or nitriles such as **2**, **7**, and **8**, and ring contraction to five-membered ring nitriles. A general ring opening reaction, leading to open-chain nitrile ylides **2**, was identified in 3-pyridylnitrene, 3-pyridylcarbene, and related molecules **1** (type I ring opening, Scheme 1).[2] In the case of 2-pyridylnitrene (**4**), 1,3-diazacycloheptatetraene (**5**) and cyanovinylketenimine (**7**) are formed on photolysis, whereas **5** together with glutacononitrile (**8**) and cyanopyrrole is formed on flash vacuum thermolysis (FVT).[3] Presumably, ring opening to diiminediyl **6a**/dienylnitrene **6b** is the source of **7** and **8** (type II ring opening, Scheme 1).[4] A similar ring opening reaction is also seen in 1-isoquinolylnitrene and other heterocyclic nitrenes.[4]

(1) (a) Wentrup, C. *Top. Curr. Chem.* **1976**, *62*, 173. (b) Wentrup, C. *Adv. Heterocycl. Chem.* **1981**, *28*. 232. (c) Wentrup, C. In *Reactive Intermediates*; Abramovitch, R. A., Ed.; Plenum Press: New York, 1980; Vol. 1, Chapter 4, p 263f. (d) Wentrup, C. In *Azides and Nitrenes*; Scrivcn, E. F. V., Ed.; Academic Press: New York, 1984; Chapter 8, p 395. (e) Gritsan, N. P.; Platz, M. S. *Adv. Phys. Org. Chem.* **2001**, *36*, 255. (f) Karney, W. L.; Borden, W. T. In *Advances in Carbene Chemistry*; Brinker, U. H., Ed.; Elsevier: Amsterdam, 2001; Vol. 3, p 205.

(2) Bednarek, P.; Wentrup, C. *J. Am. Chem. Soc.* **2003**, *125*, 9083−9089.

(3) (a) Reisinger, A.; Koch, R.; Bernhardt, P. V.; Wentrup, C. *Org. Biomol. Chem*. **2004**, *2*, 1227−1238. (b) Wentrup, C.; Winter, H.-W. *J. Am. Chem. Soc.* **1980**, *102*, 6159. (c) Crow, W. D.; Wentrup, C. *Chem. Commun.* **1969**, 1387.

10.1021/jo052541i CCC: $33.50
Published on Web 05/04/2006

SCHEME 1

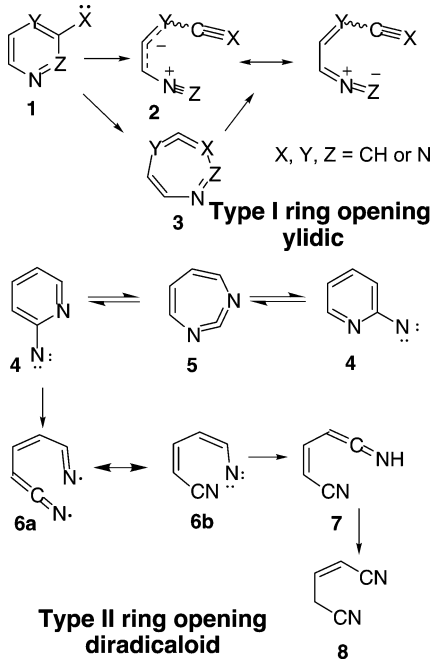

We now report our studies of 2-quinazolylnitrenes with new evidence for a diradical/nitrene route to ring opening and ring contraction as well as a photochemical interconversion of ring-expanded and ring-opened species.

Results

Tetrazole−Azide Equilibrium. Tetrazolo[1,5-*a*]quinazoline (**9**) (eq 1) was prepared from 2-chloroquinazoline and sodium azide. The compound exists exclusively as the tetrazole in the

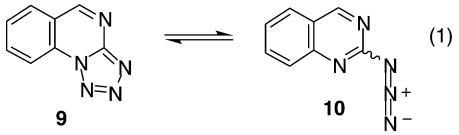

solid state and in chloroform solution at STP as evidenced by the absence of a peak near 2100 cm^{-1} in the IR spectrum. However, addition of trifluoroacetic acid to a solution in $CDCl_3$ causes the formation of the azide tautomer **10** (see eq 1) as determined by ^1H NMR spectroscopy. Thus, in a solution of $CDCl_3$−TFA (1:1), the ratio of **9** to **10** is 21:79. Gentle sublimation of the solid tetrazole **9** at 106−108 °C and condensation of the vapor with Ar to form a matrix at 20 K results in essentially the tetrazole being isolated, with only a trace of the azide. The resulting IR spectrum of the matrix is in very good agreement with the calculated spectrum of **9** (B3LYP/6-31G**; the spectra are shown in the Supporting Information, Figure S1). In contrast, sublimation of the tetrazole **9** at 200 °C and condensation with Ar afforded a totally different matrix spectrum, being essentially that of azide **10** (main peak at 2154 cm^{-1}) together with minor amounts of tetrazole **9**. Again, the experimental IR spectrum of **10** is in very good agreement with the calculated one (B3LYP/6-31G**; the spectra are shown in the Supporting Information, Figure S2).

The formation of azide **10** from tetrazole **9** on heating can be ascribed to entropy. The calculated energy difference between azide and tetrazole in the gas phase, corrected for zero-point vibrational energy, is 0.16 kcal/mol. The calculated enthalpy difference is 0.86 kcal/mol. The calculated entropy difference is 5.74 (cal/mol)/K. Thus, at 298 K, $\Delta\Delta G$(gas phase) = −0.88 kcal/mol, with the azide as the most stable form. In the crystalline state, the lattice energy is likely to stabilize the solid tetrazole. Since $\Delta G = \Delta H - T\Delta S$, increased temperature will result in a lower ΔG; i.e., it will shift the azide−tetrazole equilibrium toward the azide. This phenomenon of azide−tetrazole equilibria being governed by entropy has been established experimentally in the case of tetrazolo[1,5-*a*]-pyridines/2-azidopyridines.[5]

Nitrene 11 and the $D-\rho$ Correlation. The azide **10** was deposited in an Ar matrix at 20 K and photolyzed at either 308 or 254 nm in the cavity of an ESR spectrometer. A triplet nitrene signal developed within a few minutes in the region above 7000 G, and a half-field signal at 1468 G was observed as well (zero-field splitting parameters $D = 1.1465$ cm^{-1} and $E = 0.0064$ cm^{-1}; see Figure 1a). This signal shows distinct X_2 and Y_2 lines and therefore has a relatively large E value. This is typical of 2-pyrimidylnitrenes[6] and *s*-triazinylnitrenes,[7] where the same type of splitting is observed. This ESR spectrum is ascribed to 2-quinazolylnitrene (**11**) (Scheme 2).

There is an excellent linear correlation between the zero-field splitting parameter D and the calculated spin density ρ in a wide variety of nitrenes and carbenes.[8,9] The correlation for over 100 nitrenes is shown in Figure 2 (see also Figure S3 in the Supporting Information). The calculated natural spin density ρ of the nitrene N in **11** is 1.6279, and this data point fits very well on the $D-\rho$ correlation (see Figure 2).

The formation of **11** was confirmed by UV−vis and IR spectroscopy. The UV−vis spectrum resulting from Ar matrix photolysis of **10** at 308 nm is shown in Figure 3. The vibrational progression above 350 nm is typical of arylnitrenes.[10] The spacing of the lines between 465 and 568 nm corresponds to ca. 0.16 eV, with the main band at 529 nm. The spectrum is in good agreement with CASPT2 predictions for the triplet nitrene **11** (Figure 3).

In the IR spectrum a series of peaks between 500 and 1200 cm^{-1} can be correlated with the calculated IR spectrum of triplet nitrene **11** (Figure 4). The highest intensities of the IR and the UV−vis spectra assigned to nitrene **11** were obtained within the first minutes of irradiation and by using $\lambda = 308$ nm.

Diradical 19. Depending on the time scale of the ESR experiment, another triplet species, having the characteristics of a diradical, appeared as well (Figure 1b). This species had $D = 0.1187$ cm^{-1} and $E = 0.0026$ cm^{-1}. The diradical formed

(4) Addicott, C.; Reisinger, A.; Wentrup, C. *J. Org. Chem.* **2003**, *68*, 8538−8546.

(5) Evans, R. A.; Wong, M. W.; Wentrup, C. *J. Am. Chem. Soc.* **1996**, *118*, 4009−4017.

(6) (a) Kuzaj, M.; Lüerssen, H.; Wentrup, C. *Angew. Chem., Int. Ed. Engl.* **1986**, *25*, 480. (b) Lüerssen, H. Ph.D. Thesis, The University of Marburg, Germany, 1985.

(7) (a) Nakai, T.; Sato, K.; Shiomi, D.; Takui, T.; Itoh, K.; Kozaki, M,; Okada, K. *Mol. Cryst. Liq. Cryst.* **1999**, *334*, 157−166. (b) Chapyshev, S. V. *Mendeleev Commun.* **2002**, 168−170. (c) Chapyshev, S. V. *Mendeleev Commun.* **2003**, 53−55.

(8) Kvaskoff, D.; Bednarek, P.; George, L.; Sreekumar, P.; Wentrup, C. *J. Org. Chem* **2005**, *70*, 7947−7955 (see footnote 14).

(9) The first correlation between D values and spin densities in nitrenes was reported by Smolinsky et al.: Smolinsky, G.; Snyder, L. C.; Wasserman, E. *Rev. Mod. Phys.* **1963**, *35*, 576.

(10) Maltsev, A.; Bally, T.; Tsao, M.-L.; Platz, M. S.; Kuhn, A.; Vosswinkel, M.; Wentrup, C. *J. Am. Chem. Soc.* **2004**, *126*, 237−249.

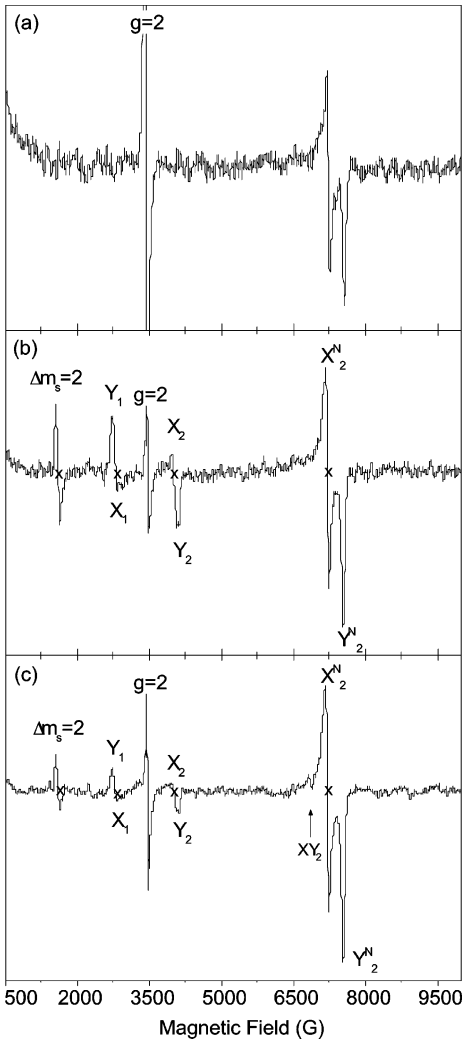

FIGURE 1. (a) ESR spectrum of **11** obtained by FVT of tetrazole **9** at 200 °C, Ar matrix isolation at 15 K, and photolysis at 308 nm (5 min). A total of 160 scans (500−10000 G), gain 8.0 × 10^5, MW frequency 9.726428 GHz (H_0 = 3470.7 G). Resonance fields: X_2, 7227.3 G; Y_2, 7552.1 G. Zero-field splitting parameters D = 1.1465 cm^{-1} and E = 0.0064 cm^{-1}. Signal at g = 2 due to adventitious doublet radical formation. (b) ESR spectrum of diradical **19** and **11** obtained by FVT of tetrazole **9** at 200 °C, Ar matrix isolation at 15 K, and photolysis at 308 nm (2 min). A total of 6 scans (500−10000 G), gain 5.0 × 10^5, MW frequency 9.727575 GHz (H_0 = 3471.1 G). Resonance fields of diradical **19**: Δm_s = 2, 1602.2 G; X_1, 2803.7 G; X_2, 4010.0 G; Y_1, 2715.7 G; Y_2, 4090.6 G. D = 0.1187 cm^{-1}, E = 0.0026 cm^{-1}. Resonance fields of nitrene **11**: X^N_1, 7213.9 G; Y^N_2, 7538.7 G. D = 1.1413 cm^{-1}, E = 0.0064 cm^{-1}. (c) ESR spectrum of diradical **19**, **11**, and a minor nitrene, possibly **18** or (*Z*)-**20**, obtained from FVT of tetrazole **9** at 200 °C, Ar matrix isolation at 15 K, and photolysis at 308 nm (6 min). A total of 32 scans (500−10000 G), gain 5.0 × 10^5, MW frequency 9.727535 GHz (H_0 = 3471.1 G). Resonance fields of diradical **19**: Δm_s = 2, 1599.7 G; X_1, 2803.7 G; X_2, 4010.0 G; Y_1, 2735.3 G; Y_2, 4117.5 G. D = 0.1187 cm^{-1}, E = 0.0027 cm^{-1}. Resonance fields of nitrene **11**: Δm_s = 2, 1460.6 G; X^N_1, 7211.5 G; Y^N_2, 7538.7 G. D = 1.1408 cm^{-1}, E = 0.0065 cm^{-1}. Resonance fields of the minor nitrene: X_1, 6850.1 G; Y_2, 6894.0 G. D = 0.9474 cm^{-1}, $E \leq$ 0.0009 cm^{-1}.

slower than nitrene **11**, but it was thermally unstable, even at 15 K. The diradical did not appear at all if the scanning time of the spectrometer (200 s per scan) exceeded its lifetime. Thus, it does not appear in Figure 1a (160 scans) but in Figure 1b (6 scans) (see also Figures S4 and S5 in the Supporting Information). The disappearance of the diradical followed first-order kinetics with $t_{1/2} \approx$ 47 min at 15 K in the dark (see Figure S6, Supporting Information). This spectrum is assigned to one or more of the conformers of the diradical **19** (Scheme 2), which would form on ring opening of either nitrene **11** or the ring-expanded triazacycloheptatetraene **14** (Scheme 2). All three conformers of the triplet diradical (**19a**−**c**) are computational energy minima (see below). Although one of the mesomeric structures of each conformer of **19** is a nitrene, this has little weight because it is an *o*-quinoid, and therefore, the ESR spectrum does not look like that of a nitrene (the calculated natural spin densities on the three nitrogen atoms in **19b** are 1.027, 0.461 (−*N*CN), and 0.314 (−NC*N*), and in **19c** 1.074, 0.450, and 0.309. The decay of the ESR signal of **19** is ascribed to intersystem crossing to the open-shell singlet, which has a very low barrier for transformation to the end products **21** and **22** (energy difference between triplet **19T** and open-shell singlet **19OSS**, 1−2 kcal/mol; activation barrier for **19bOSS** → **21**, 1.3 kcal/mol at the CASSCF(8,8) level; see the Calculations).

SCHEME 2

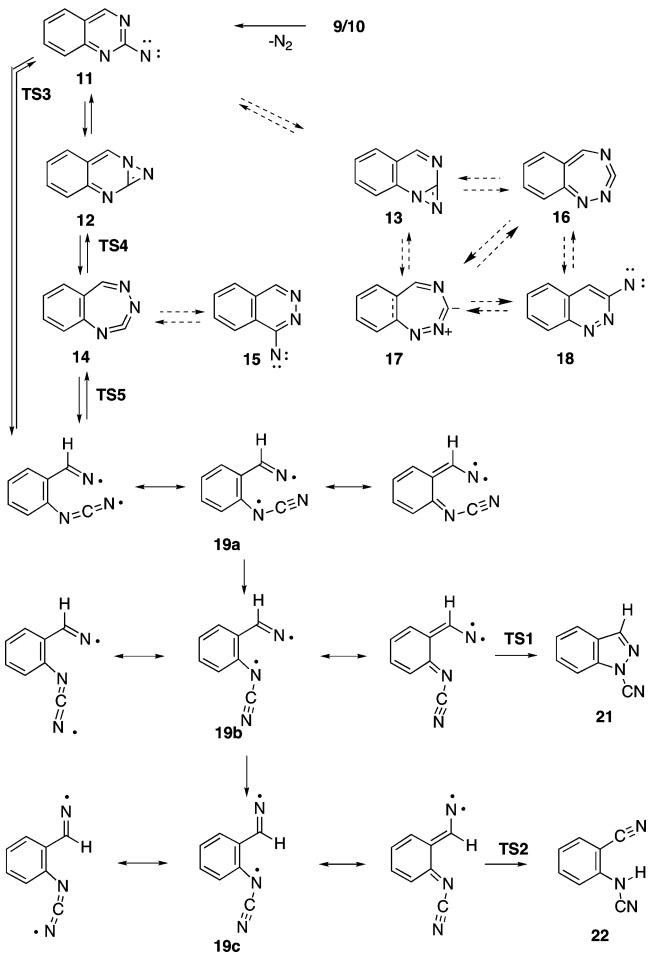

The concentration and/or the extinction coefficients of the bands of the diradical **19** were too low for its secure identification by IR and UV−vis spectroscopy.

Minor Nitrene. A third triplet species giving rise to a weak XY_2 signal near 6900 G was also detected in the ESR spectra following photolysis at 308 nm (Figure 1c; see also Figures S4 and S5). This signal was relatively stronger when 254 nm photolysis was used. This species has D = 0.9587 cm^{-1} and $E \leq$ 0.0008 cm^{-1}. The rates of formation and disappearance of

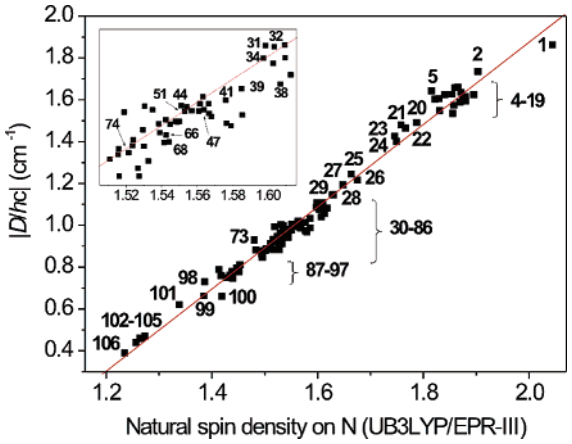

FIGURE 2. Correlation between the zero-field splitting parameter $|D/hc|$ (cm^{-1}) and natural spin density ρ for triplet nitrenes, NR, calculated at the UB3LYP/EPRIII level. Hereafter the splitting parameter $|D/hc|$ is usually referred to as D. The correlation fits the equation $D = 1.96673\rho - 2.0577$ cm^{-1} with standard deviation on $D = \pm 0.04$ cm^{-1}. $R^2 = 0.993$ for all data. This figure is shown on a larger scale, and the data for D and ρ and the references are listed in the Supporting Information. Key for nitrene substituent R: 1, H; 2, trifluoromethyl; 3, triphenylmethyl; 4, α-carbethoxybenzyl; 5, 2-methyl-*o*-carboran-1-yl; 6, diphenylmethyl; 7, 1-azido-1-phenylmethyl; 8, *tert*-butyl; 9, 1-azido-1,1-diphenylmethyl; 10, 2-octyl; 11, *n*-propyl; 12, 9-azido-9*H*-fluoren-9-yl; 13, *o*-carboran-1-yl; 14, (*eq*)-cyclohexyl; 15, methyl; 16, adamantyl; 17, cyclopentyl; 18, norbornyl; 19, *o*-carboran-9-yl; 20, (*o*-phenylenedioxy)boranyl; 21, 4-azido-6-dimethylamino-*s*-triazin-2-yl; 22, 4,6-bis(dimethylamino)-*s*-triazin-2-yl; 23, 4,6-dimethoxy-*s*-triazin-2-yl; 24, 4,6-diazido-*s*-triazin-2-yl; 25, 4,6-dimethylpyrimidin-2-yl; 26, 2-pyrimidyl; 27, 4-pyrimidyl; 28, 4-phenyl-2-quinazolyl; 29, 2-quinazolyl; 30, 3,5-bis(trifluoromethyl)-2-pyridyl; 31, 4-pyridyl; 32, 3-pyridazinyl; 33, 5-trifluoromethyl-2-pyridyl; 34, 2,3,5,6-tetrafluoro-4-pyridyl; 35, 4-trifluoromethyl-2-pyridyl; 36, 3-trifluoromethyl-2-pyridyl; 37, 6-trifluoromethyl-2-pyridyl; 38, 2-pyridyl; 39, 2-quinolyl; 40, 4,6-dimethylpyridazin-3-yl; 41, 2-pyrazinyl; 42, 3-biphenylyl; 43, 4-fluorophenyl; 44, 3-pyridyl; 45, 4-(*N*-methylacetamido)phenyl; 46, 2-(trifluoromethyl)phenyl; 47, phenyl; 48, 4-methoxyphenyl; 49, 3-tolyl; 50, 3-aminophenyl; 51, 4-quinazolyl; 52, 2-biphenylyl; 53, 3-dimethylaminophenyl; 54, 3-nitrophenyl; 55, 4-azidobiphenyl-3′-yl; 56, 4-carboxyphenyl; 57, 4-tolyl; 58, 4-nitrophenyl; 59, 4-ethylphenyl; 60, 3-carboxyphenyl; 61, 4-hydroxyphenyl; 62, 3,5-diazido-2,4,6-tricyanobenzen-1-yl; 63, 3-methoxyphenyl; 64, 2-(*n*-butyl)phenyl; 65, 4-cyanophenyl; 66, 2-quinoxalyl; 67, 4-(acetylamino)phenyl; 68, 3-isoquinolyl; 69, 4-carbethoxyphenyl; 70, 4-biphenylyl; 71, 7-azido-2-phenanthrenyl; 72, 4-azidophenyl; 73, 4-(phenylethynyl)phenyl; 74, 2-naphthyl; 75, 6-phenanthridinyl; 76, 7-azido-3-dibenzofuranyl; 77, 4-acetylphenyl; 78, 3-azidobiphenyl-4′-yl; 79, 2-fluorenyl; 80, 4′-azido[1,1′-biphenyl]-4-yl; 81, 2′-cyano-2-biphenylyl; 82, 4-quinolyl; 83, 9-oxo-9*H*-fluoren-2-yl; 84, 7-azido-9*H*-fluoren-2-yl; 85, 7-azido-9-oxo-9*H*-fluoren-2-yl; 86, 1-isoquinolyl; 87, 9-phenanthryl; 88, (*E*)-[4-[2-(4-azidophenyl)vinyl]phenyl]; 89, 1-naphthyl; 90, 8-methyl-1-naphthalenyl; 91, 8-nitro-1-naphthalenyl; 92, 8-carboxy-1-naphthalenyl; 93, 2-anthryl; 94, (*E*)-[4-[2-(4-aminophenyl)vinyl]phenyl]; 95, 8-azido-1-naphthalenyl; 96, 8-hydroxy-1-naphthalenyl; 97, (*E*)-[4-[(4-azidophenyl)azo]phenyl]; 98, 1-pyrenyl; 99, 1-anthryl; 100, (*E*,*E*)-[4-[4-(4-azidophenyl)-1,3-butadienyl]phenyl]; 101, 8-amino-1-naphthalenyl; 102, 9-anthryl; 103, 10-methoxy-9-anthryl; 104, 10-phenyl-9-anthryl; 105, 10-nitro-9-anthryl; 106, 10-cyano-9-anthryl.

the three triplet species are different, but the low intensity of the ESR signal at 6900 G makes the identification of its carrier tentative. Two nitrenes isomeric with **11**, viz., 1-phthalazinylnitrene (**15**) or 3-cinnolinylnitrene (**18**) (Scheme 2), need to be considered. These are annelated derivatives of 3-pyridazinylnitrene, which we have observed previously (see Figure 2),[8] and they would be expected to give rise to XY_2 lines in the ESR spectrum. Nitrenes **15** and **18** have calculated natural spin

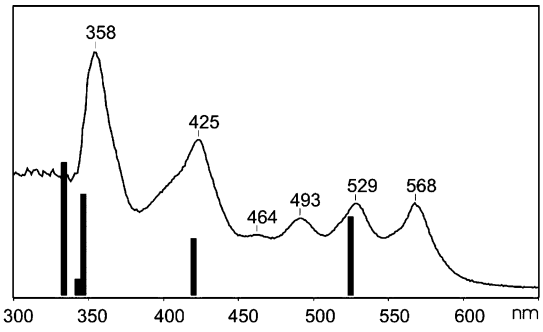

FIGURE 3. UV−vis spectrum of nitrene **11** formed on photolysis of azide **10** in an Ar matrix at 10 K using $\lambda = 308$ nm. Heavy bars are CASPT2-calculated transitions for triplet **11**.

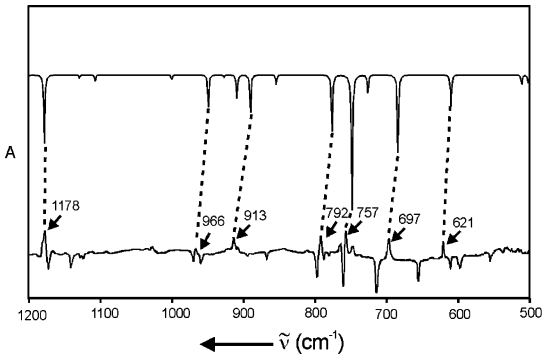

FIGURE 4. (Top) calculated (B3LYP/6-31G**) and (bottom) experimental IR spectra of triplet nitrene **11** obtained by photolysis of azide **10** in an Ar matrix at 10 K using $\lambda = 308$ nm.

densities on the nitrene N, $\rho = 1.5124$ and 1.5395, respectively, and on this basis they would be expected to have D values near 0.91 and 0.97 cm^{-1}, respectively. **18** fits well on the $D-\rho$ correlation (Figure 2), so the weak signal observed at 6900 G (Figure 1c) could be due to **18**, formed via **13**, **16**, and/or **17**, although **15** cannot be ruled out (the standard deviation on D for all data in Figure 2 is ± 0.04 cm^{-1}).

The phenylnitrene derivative **20** has to be considered as another possible source of the weak 6900 G signal. This nitrene could be formed by alternate ring opening of **11** (eq 2), and it

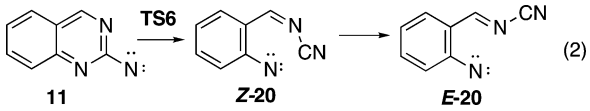

can exist in *Z* and *E* forms, both of which are calculated energy minima in the triplet state. The calculated natural spin density on the nitrene N in (*Z*)-**20** is 1.5152, and in (*E*)-**20** it is 1.4804. The value for (*E*)-**20** is rather too low for this nitrene to be considered; however, the value for (*Z*)-**20** fits on the $D-\rho$ correlation (predicted $D = 0.92$ cm^{-1}). Therefore, **18** and (*Z*)-**20** remain as plausible candidates for the minor nitrene, with **15** as a further possibility. The formation of nitrene **34** in Scheme 3 makes (*Z*)-**20** the strongest contender for the minor nitrene. The formation of nitrene **20** corresponds to a type II ring opening (cf. Scheme 1). If **20** is formed, it could be expected to ring close again to **11**, **13**, **16**, or **17**, or it could give rise to a small amount of 2-cyanoindazole. This has a calculated CN stretching vibration 11 cm^{-1} higher than that of 1-cyanoindazole (**21**). Weak signals at 2271−2277 cm^{-1} in

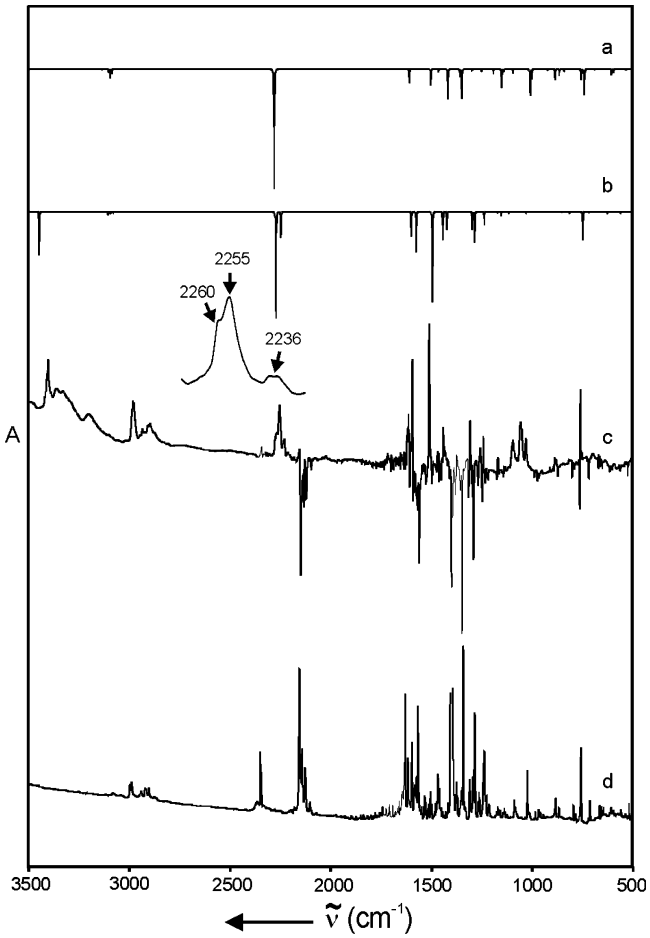

FIGURE 5. (a) Calculated IR spectrum of **21**, (b) calculated IR spectrum of *anti*-**22**, (c) difference IR spectrum resulting from exhaustive photolysis of azide **10**/tetrazole **9** (negative peaks) at 254 nm in an Ar matrix at 10 K (inset: detail showing peaks due to **21** (2260 cm^{-1}) and **22** (2255 and 2236 cm^{-1})), and (d) IR spectrum of azide **10**/tetrazole **9** deposited in an Ar matrix at 10 K. Calculations are at the B3LYP/6-31G* level.

many of the IR spectra where **21** is present (2260 cm^{-1}; see below) could therefore possibly be due to traces of 2-cyanoindazole.

Ring Opening and Ring Contraction to 21 and 22. Photolysis of an Ar matrix of azide **10** at ca. 10 K at 308, 254, or 222 nm with FTIR detection caused conversion of any remaining tetrazole to azide, conversion of the azide to the nitrene (best observed by photolyzing at 308 nm; see above), and finally disappearance of the nitrene **11** with concomitant formation of two new nitriles showing absorptions in the 2230−2260 cm^{-1} range and NH absorption around 3410 cm^{-1} in the IR spectrum (Figure 5). The carrier of this spectrum is identified as a mixture of **21** and the *anti* form of *N*-cyanoanthranilonitrile (**22**) (see Scheme 2). Careful monitoring of the photolyses revealed that **21** is formed more rapidly than **22**. Thus, for the first minutes of photolysis at 308 nm, only **21** was detectable. Compound **21** was identified by direct comparison with samples prepared from indazole and BrCN and by FVT of **9**/**10** (see below and Figure S11 in the Supporting Information). Important wavenumbers of **21** are 2260 (CN), 1507, 1429, 1373, 1027, 908, 748, and 746 cm^{-1}. Compound **22** was identified on the basis of comparison with a previous investigation of this compound[11] as well as the good agreement with the IR spectrum calculated at the B3LYP/6-31G* level (Figure 5). Important experimental wavenumbers of **22** are 3411/3406, 2255 (NHCN), 2236 (CN), 1595, 1511, 1439, 1306, 1256, 1167, and 757 cm^{-1}. The calculated IR spectrum of the corresponding *syn* form of **22** shows a less satisfactory agreement (Figure S7). The *anti* form of **22** is stabilized by a hydrogen bond between NH and the *o*-cyano group. Other compounds that can be excluded on the basis of comparison with the calculated spectra are *N*-(2-cyanophenyl)carbodiimide (2-NC−C_6H_4−N=C=NH) and (2-isocyanophenyl)diazomethane (2-CN−C_6H_4−CH=N_2) (see Figures S8 and S9 in the Supporting Information).

In addition to compounds **21** and **22**, a very small peak at 1990 cm^{-1}, shown in Figure S10 in the Supporting Information and not visible in Figure 5, is suggestive of formation of a trace of the ring-expanded carbodiimide 1,3,4-triazabenzo[*e*]cycloheptatetraene (**14**) (calculated value 1994 cm^{-1}, very strong, Figure S10). The position of this peak is characteristic of seven-membered cyclic carbodiimides of this type.[7c,12,13] The alternative, higher energy *o*-quinoid isomer **16** has a calculated strong absorption at 1938 cm^{-1} and was not observed (the calculated spectrum is shown in Figure S14 in the Supporting Information). The zwitterionic isomer **17**, which can be regarded as a cyclic nitrile imine,[8,10,12] was also not observed. The highest calculated vibrational frequencies of this molecule are in the 1500−1600 cm^{-1} range (Figure S15 in the Supporting Information). The diazirenes **12** and **13** have calculated $\nu_{C=N}$ at 1745 and 1707 cm^{-1}, respectively, and were not observed (the calculated IR spectra of **12** and **13** are shown in Figures S12 and S13 in the Supporting Information). The formation of **11**, **14**, and **19** is summarized in Scheme 2 and will be discussed further below. The two facile reaction routes of diradical **19**, leading to **21** and **22** (Scheme 2), readily explain the instability of the diradical observed in the matrix by ESR spectroscopy (see the Calculations).

Flash Vacuum Thermolysis to 21. Preparative FVT of tetrazole **9**/azide **10** at 500−700 °C afforded **21** as the main product. This compound was isolated from the FVT reaction, purified by chromatography, and characterized by elemental analysis, comparison with a sample prepared from indazole and cyanogen bromide, and the excellent agreement with the calculated IR spectrum (Figure S11).

GC−MS analysis of the FVT products obtained at 430−600 °C revealed the presence of tetrazole **9** up to 500 °C as well as the formation of 2-aminoquinazoline (**23**) (11% at 430 °C, 35% at 600 °C), **21** (28% at 430 °C, 65% at 600 °C), and a trace of indazole (**24**) (0.6−1.8%) (see eq 3). The formation of amines

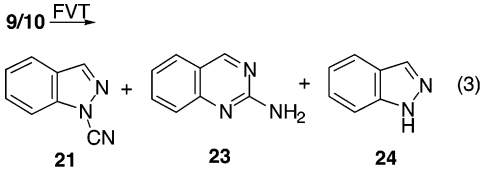

such as **23** is characteristic of triplet (hetero)arylnitrenes, even in low-pressure gas-phase reactions.[8] Substantial amounts of

(11) (a) Vosswinkel, M. Ph.D. Thesis, The University of Queensland, Australia, and Universität Bochum, Germany, 2002. (b) Wentrup, C. *Tetrahedron* **1971**, *27*, 367−374.

(12) Kuhn, A.; Vosswinkel, M.; Wentrup, C. *J. Org. Chem.* **2002**, *67*, 9023−9030.

(13) Bucher, G.; Siegler, F.; Wolff, J. J. *Chem. Commun.* **1999**, 2113−2114.

SCHEME 3

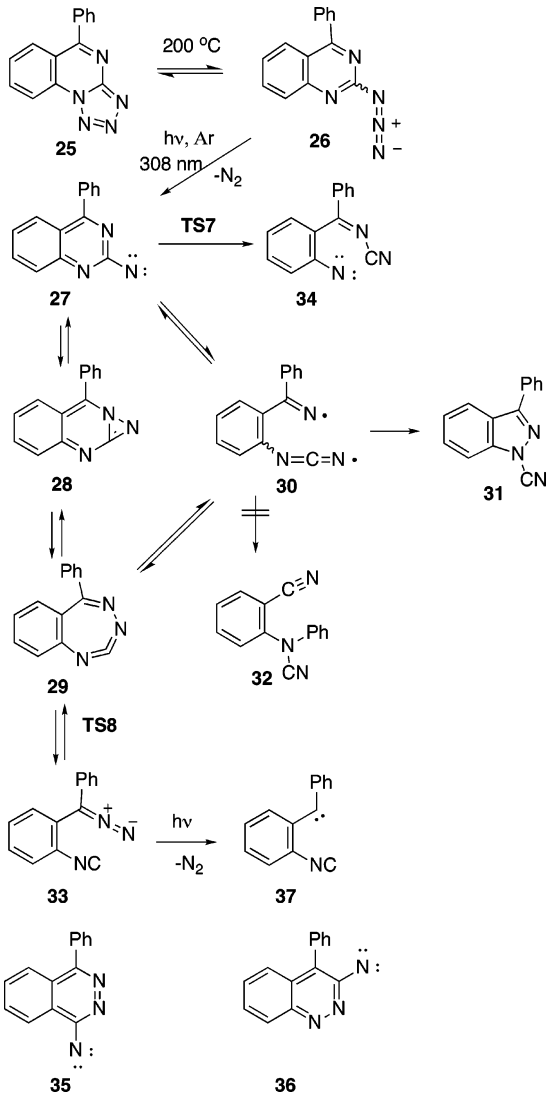

2-aminopyrimidines were also seen in the FVT reactions of 2-pyrimidylnitrenes.[14]

FVT of **9**/**10** at 500 °C using the external oven (see the Experimental Section) and Ar matrix isolation of the product afforded the IR spectrum of **21** (Figure S11). The less volatile 2-aminoquinazoline and tetrazole **9** would have condensed in the air-cooled part of the thermolysis tube and not reached the matrix isolation window under these conditions.

4-Phenyl Derivative 25/26. Reversible Ring Expansion to 29 and Ring Opening to Diazoalkane 33. Sublimation of 6-phenyltetrazolo[1,5-*a*]quinazoline (**25**) through a hot tube at 200 °C and Ar matrix isolation of the vapor at 10 K afforded the azide valence tautomer **26**, characterized by strong bands at 2137, 2131, and 1327 cm^{-1} (Figure 6a). Preparative FVT of **25/26** at 380 °C afforded 1-cyano-3-phenylindazole (**31**) in 63% isolated yield. It was identified by elemental analysis, the presence of a strong CN stretching vibration at 2255 cm^{-1}, and hydrolysis to 3-phenylindazole in hot NaOH.

Photolysis of Ar matrix isolated **26** at 308 nm in the ESR cryostat at 15 K caused the appearance of a strong ESR spectrum

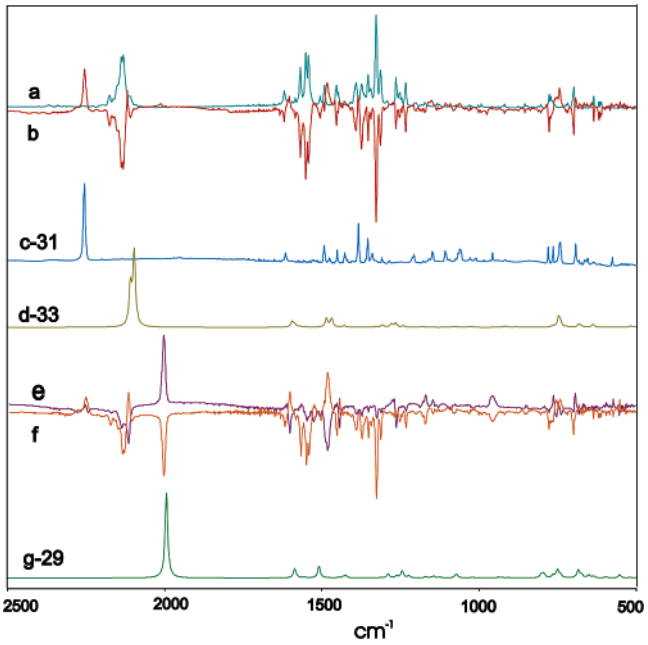

FIGURE 6. (a) IR spectrum of azide **26** isolated in an Ar matrix at 10 K, (b) result of photolysis at $\lambda = 310-390$ nm (photolysis at 313 nm gives the same result), (c) IR spectrum of nitrile **31** deposited in Ar at 10 K, (d) calculated IR spectrum of **33**, (e) result of photolysis of the matrix from (b) at $\lambda > 475$ nm, (f) result of photolysis of the matrix from (e) at 310−390 or 313 nm, and (g) calculated IR spectrum of **29**. Calculations are at the B3LYP/6-31G* level.

(Figure S18 in the Supporting Information) very similar to that of **11** shown in Figure 1a. It is therefore ascribed to triplet nitrene **27** ($D = 1.147$ cm^{-1}, $E = 0.0060$ cm^{-1}). A diradical like **19** (**30**) was not observed. However, another weak nitrene signal developed very slowly as well (XY_2 at 7039 G, $H_0 = 3471.1$ G, frequency 9.7280 GHz, $D = 1.0163$ cm^{-1}, $E < 0.001$ cm^{-1}). This second nitrene is probably due to a ring opening of the quinazoline ring to give the arylnitrene **34** rather than the phthalazinyl- and cinnolinylnitrenes (**35** and **36)** (Scheme 3). (*Z*)-**34** is analogous to nitrene (*Z*)-**20**. The *D* value near 1.0 cm^{-1} is characteristic of phenylnitrenes (cf. Figure 2), and nitrene (*Z*)-**34** fits much better on the $D-\rho$ correlation than does **35** or **36** (the expected *D* values for these three nitrenes are 0.98, 0.78, and 0.91 cm^{-1}, respectively.

Photolysis of azide **26** at 313 or 310−390 nm in the IR cryostat led to the disappearance of the azide absorption at 2131 cm^{-1} and the formation of three new compounds absorbing at 2006 (A), 2120/2142 (B), and 2256 (C) cm^{-1} (Figures 6b, 6e, and 6f). Compound A is assigned as the triazacycloheptatetraene **29** because of the good agreement with its calculated IR spectrum (the calculated carbodiimide stretch is 1994 cm^{-1}, Figure 6g). Compound C is **31**, as verified by separate deposition of this compound (Figure 6c). Compound B is assigned as the (*o*-isocyanophenyl)diazomethane **33** because of the good agreement with the calculated spectrum (2097 (NC) and 2109 (CN_2) cm^{-1}, Figure 6d) and the reversible interconversion with **29** (Figure 6e,f). Thus, compound B (**33**; 2120/2142 cm^{-1}) is bleached at $\lambda > 475$ nm, and compound A (**29**; 2006 cm^{-1}) is formed in its place. Continued photolysis at 310 nm causes the bleaching of the 2006 cm^{-1} absorption (**29**) and regeneration of diazo compound **33** at 2120/2142 cm^{-1}. This process cannot be repeated indefinitely because the bleaching of **29** also results in increased intensity of the cyanoindazole **31** (2256 cm^{-1}) (see

(14) Wentrup, C.; Crow, W. D. *Tetrahedron* **1970**, *26*, 4915−4924. Wentrup, C.; Crow, W. D. *Tetrahedron* **1971**, *27*, 1566.

TABLE 1. Calculations on Nitrene 11, Diradicals 19a−c, and Relevant Intermediates and Transition States[a]

species[b]	CASSCF(8,8)/6-31G*	CASPT2	UB3LYP/6-31G* [c]
11T	0	0	0
11OSS	19.6	21.3	
12	39.6	56.9	33.2
13	36.5	21.0	21.6
12 → 14 (**TS4**)			37.4
14	26.1	14.3	11.2
19aOSS	35.4	31.3	24.2
19aCSS at OSS geometry	104.6	98.1	50.8
19aT	34.0	29.3	21.4
14 → 19aOSS (**TS5**)	45.0	35.4	
11T → 19aT (**TS3**)			28.8
11T → (*Z*)-20T (**TS6**)			34.2
19bOSS	26.7	24.7	18.9
19bCSS at OSS geometry	90.4	82.6	45.9
19bT	24.4	22.3	16.1
19bOSS → 21 (**TS1**)	28.0		
19cOSS	22.4	21.1	15.9
19cCSS at OSS geometry	94.3	90.2	43.9
19cT	21.0	19.0	13.3

[a] Energies relative to that of triplet **11T** in kilocalories per mole. [b] T = triplet, OSS = open-shell singlet, and CSS = closed-shell singlet. [c] In the UB3LYP calculations the OSS energies are estimated by the Ziegler−Cramer method.[18]

Figure 6f). Compounds **29** and **33** have similar calculated energies, 2.95 and −0.13 kcal/mol, respectively, with respect to that of the triplet nitrene **27T** (without the phenyl substituents they are 11.2 and 7.7 kcal/mol, respectively, with respect to that of nitrene **11T**). The calculated transition structure between **29** and **33** (**TS8**, Scheme 3) lies 53.4 kcal/mol above **33**.

Phenyldiazomethanes are usually red. The Ar matrixes containing **33** are visibly red. They are formed by photolysis of azide **26** at 313 nm and feature a broad maximum at 510−550 nm in the UV−vis spectrum (Figure S19 in the Supporting Information). The calculated λ_{max} for **33** is 513 nm (time-dependent B3LYP/6-31G*). This absorption is bleached at $\lambda > 475$ nm and regenerated on photolysis at 313 nm. Thus, as in the IR spectra, the visible absorption at 510−550 nm is ascribed to diazo compound **33**, which on bleaching gives triazacycloheptatetraene **29**. The latter has no calculated absorption in the visible spectrum. The experimental UV−vis spectra and calculated transitions are presented in the Supporting Information.

The photolysis of diazo compounds usually leads to the formation of carbenes. Indeed, on photolysis of **26** at 308 nm, apart from the formation of nitrene **27** and the minor nitrene mentioned above, weak signals ascribed to *o*-(isocyanophenyl)-phenylcarbene (**37**) (see Scheme 3) were observed (X_2 at 4823.7 G, Y_2 at 5576.7 G, H_0 = 3471.2 G, frequency 9.7280 GHz, D = 0.4053 cm^{-1}, E = 0.0192 cm^{-1}). For comparison, diphenylcarbene has D = 0.4050 cm^{-1} and E = 0.0186 cm^{-1}.[15]

Calculations

The energies and IR spectra of the relevant species in Schemes 2 and 3 were calculated at the (U)B3LYP/6-31G* or (UB)3LYP/6-31G** level using the Gaussian 03 suite of programs.[16] Energies (E) were corrected for zero-point vibrational energies (ZPEs), and all wavenumbers were scaled by a factor of 0.9613.[17] Relative E + ZPE: triplet 2-quinazolylnitrene (**11T**), 0 (absolute E + ZPE = −471.906769 hartrees); **12**, 33.2; **13**, 21.6; **14**, 11.2; triplet nitrene **15T**, 19.7; **16**, 33.6; **17**, 40.7; triplet nitrene **18T**, 20.8; triplet **19aT**, 21.4; triplet **19bT**, 16.1; triplet diradical **19cT**, 13.3; triplet nitrene (*Z*)-**20T**, 25.4; triplet nitrene (*E*)-**20T**, 19.7; **21**, −26.4; 2-cyanoindazole, −17.6; *syn*-**22**, −29.6; *anti*-**22**, −36.2; (2-cyanophenyl)-carbodiimide, −36.4; (2-isocyanophenyl)diazomethane, 7.72 kcal/mol. Relative E + ZPE: triplet nitrene **27T**, 0 (absolute E + ZPE = −702.877843 hartrees); **34T**, 21.62; **28**, 2.95; **33**, 0.13 kcal/mol.

The transition structures for the following reactions were also calculated at the (U)B3LYP/6-31G* level. Energies of transition structures are relative to that of **11T** (0): **11T → 19aT** (**TS3**, Scheme 2), 28.8; **11T → (*Z*)-20T**, 34.2; **12 → 14**, 37.4; **14 →** (*o*-isocyanophenyl)diazomethane, 57.0 kcal/mol. The following transition structure energies are relative to that of **27T** (0): **27T → 34T** (**TS7**), 34.6; **29 → 33** (**TS8**), 53.4 kcal/mol.

The energies of the triplet ground states **19a−cT**, open-shell singlets **19a−cOSS**, and corresponding closed shells **19a−cCSS** were calculated at the CASSCF(8,8)/6-31G* level (active space consisting of one σ and seven π orbitals). Relative energies are presented in Table 1. Full details are given in the Supporting Information. The energies of the OSSs were only 1−2 kcal/mol above those of the triplets. Therefore, intersystem crossing will be very facile, even at 15 K, where the triplets were found to decay (Figure S6). The energies of the closed-shell singlet diradicals **19a−cCSS** were calculated at the OSS geometries and were found to be 69.2, 63.7, and 71.9 kcal/mol above those of the OSSs, respectively, at the CASSCF level, 66.8, 57.9, and 69.1 kcal/mol above those of **19a−cOSS**, respectively, at the CASPT2 level, and 26−28 kcal/mol above those of the OSSs according to the UB3LYP estimates using the Ziegler−Cramer sum method[18] for calculating OSS energies (Table 1). Thus, clearly, the chemically interesting

(15) Brandon, R. W.; Closs, G. L.; Hutchison, C. A., Jr. *J. Chem. Phys.* **1962**, *37*, 1878.

(16) Frisch, M. J.; Trucks, G. W.; Schlegel, H. B.; Scuseria, G. E.; Robb, M. A.; Cheeseman, J. R.; Montgomery, J. A., Jr.; Vreven, T.; Kudin, K. N.; Burant, J. C.; Millam, J. M.; Iyengar, S. S.; Tomasi, J.; Barone, V.; Mennucci, B.; Cossi, M.; Scalmani, G.; Rega, N.; Petersson, G. A.; Nakatsuji, H.; Hada, M.; Ehara, M.; Toyota, K.; Fukuda, R.; Hasegawa, J.; Ishida, M.; Nakajima, T.; Honda, Y.; Kitao, O.; Nakai, H.; Klene, M.; Li, X.; Knox, J. E.; Hratchian, H. P.; Cross, J. B.; Bakken, V.; Adamo, C.; Jaramillo, J.; Gomperts, R.; Stratmann, R. E.; Yazyev, O.; Austin, A. J.; Cammi, R.; Pomelli, C.; Ochterski, J. W.; Ayala, P. Y.; Morokuma, K.; Voth, G. A.; Salvador, P.; Dannenberg, J. J.; Zakrzewski, V. G.; Dapprich, S.; Daniels, A. D.; Strain, M. C.; Farkas, O.; Malick, D. K.; Rabuck, A. D.; Raghavachari, K.; Foresman, J. B.; Ortiz, J. V.; Cui, Q.; Baboul, A. G.; Clifford, S.; Cioslowski, J.; Stefanov, B. B.; Liu, G.; Liashenko, A.; Piskorz, P.; Komaromi, I.; Martin, R. L.; Fox, D. J.; Keith, T.; Al-Laham, M. A.; Peng, C. Y.; Nanayakkara, A.; Challacombe, M.; Gill, P. M. W.; Johnson, B.; Chen, W.; Wong, M. W.; Gonzalez, C.; Pople, J. A. *Gaussian 03*, revision C.01; Gaussian, Inc.: Wallingford, CT, 2004.

(17) Wong, M. W. *Chem. Phys. Lett.* **1996**, *256*, 391−399.

(18) Johnson, W. T. G.; Sullivan, M. B.; Cramer, C. J. *Int. J. Quantum Chem.* **2001**, *85*, 492−508.

diradicals are the triplets and the open-shell singlets. Attempts to optimize the geometries of **19a**−**cCSS** invariably resulted in rearrangement to **21** or **22**, which suggests that the activation barriers for these processes are not high. The transition structure for the ring closure of diradical **19bOSS** to **21** (**TS1**, Scheme 2) was obtained at the CASCF(8,8)/6-31G* level and lies a mere 1.3 kcal/mol above **19bOSS** (imaginary frequency 237 cm^{-1}). A transition structure for the hydrogen shift **19c** → **22** (**TS2**, Scheme 2) could not be located, but this energy surface is quite flat at the CASSCF(8,8) level, and the activation barrier is therefore expected to be very low. Thus, the low calculated singlet−triplet splittings (**19OSS**−**19T**), the low barrier for the cyclization **19bOSS** → **21** (**TS1**), and the suggested low barrier for **19c** → **22** (**TS2**) are in good agreement with the transient nature of **19a**−**cT**, which disappear in the Ar matrix with a half-life of ca. 47 min (Figure S6).

The transition structure for the ring opening of the closed-shell singlet cyclic carbodiimide **14** to the open-shell singlet diradical **19aOSS** (**TS5**, Scheme 2) was also calculated at the CASSCF-(8,8)/6-31G* and CASPT2 levels (Table 1, 18.9 and 21.1 kcal/mol, respectively, relative to the energy of **14**).

The UV−vis spectrum of triplet nitrene **11** was predicted by using CASPT2 calculations (wavelengths, oscillator strengths): 517 nm, 0.013164; 416 nm, 0.009554; 345 nm, 0.002519; 346 nm, 0.016812; 299 nm, 0.010211; 336 nm, 0.021898; 285 nm, 0.009309. The UV−vis spectra of **29** and **33** were calculated by using density functional theory based on time-dependent (TD) response theory.[19] We used the TD-DFT implementation in Gaussian 98 as described recently by Stratmann et al.[20]

Natural and Mulliken spin densities in nitrenes and diradicals were calculated using UB3LYP/EPRIII within Gaussian 03.[21] Zero-field splitting parameters *D* and *E* (cm^{-1}) were calculated from experimental ESR spectra using Wasserman's equations.[22]

Discussion

Schemes 2 and 3 summarize the observations and provide a general explanation for the results. Ring expansion could in principle take place in two ways, via **12** to **14** or via **13** to **16**. If the ring expansions were fully reversible, nitrenes **15** and **18** could also be formed. As described above, the measured zero-field splitting parameter *D* is in agreement with **11** as the main triplet species observed by matrix ESR spectroscopy.

Furthermore, a triplet diradical was formed within the first few minutes of photolysis, and it was assigned the structure **19T** on the basis of its ESR spectrum. The three conformers **19a**−**c** are all calculated energy minima, but the *Z*-conformer **19a** has a slightly nonplanar arrangement of the two *ortho* substituents for steric reasons. **19c** has the lowest energy, followed by **19b** and **19a**. The initial optimization of **19a** led to ring closure to the triazacycloheptatrienylidene benzo[*e*]-1,2,4-triazepin-3-ylidene (44.8 kcal/mol above triplet **11b**), but reoptimization led to the nonplanar **19a** (21.5 kcal/mol above triplet **11**). Three mesomeric structures are shown for each of **19a**−**c** in Scheme 2, whereby the structures with an (H)C═N double bond have the highest weight and the structures with an (H)C−N single bond (nitrene) have the lowest. The calculated structures of **19a**−**c** all have delocalized CNCN moieties.

The observed triplet diradical **19** was thermally unstable and decayed with first-order kinetics at 15 K (Figure S6). According to the CASSCF(8,8) calculations, this is most likely due to the facile intersystem crossing to the open-shell singlet diradicals **19a**−**cOSS** (energies 1−2 kcal/mol above those of **19a**−**cT**), which have very low activation barriers for transformation to the end products **21** and **22** (1.3 kcal/mol for **19bOSS** → **21** (**TS1**, Scheme 2); see the Calculations). The direct transformations of triplet **19a**−**c** to **21** or **22** would be spin-forbidden processes.

We have observed diradicals by ESR spectroscopy in Ar matrix photolyses of other tetrazoles and azides, e.g., in the reactions leading to 1-quinolyl-, 3-quinolyl-, and 2-naphthylnitrenes (*D* (*E*) values (cm^{-1}) of the diradicals: 0.0429 (0.0073), 0.0869 (0.003), and 0.0223 (0.0000), respectively). All these diradicals are assumed to be formed by type II ring opening (see Scheme 1).[6b]

Neither of the possible diazirenes **12** and **13** was observed in the matrix IR spectra. This is not surprising: the calculated transition structure for the exothermic reaction **12** → **14** lies only 4 kcal/mol above **12** at the B3LYP/6-31G* level. As expected, due to the *o*-quinoid structure of the triazacycloheptatetraene **16**, the calculated energy of **14** is lower than that of **16** (11.2 vs 33.6 kcal/mol relative to that of the triplet nitrene **11**), and **16** was not observed. For the same reason, the energy of diazirene **12** is higher than that of **13** (see Table 1). The energy splitting between the ground-state triplet and the open-shell singlet state in phenylnitrenes is on the order of 18−20 kcal/mol.[1e,f,8,10,23] For **11**, it is calculated as ca. 20 kcal/mol (Table 1). Thus, the CASPT2 and B3LYP calculations predict that the formation of triazacycloheptatetraene **14** is exothermic from the singlet nitrene **11**, but the formation of the *o*-quinoid diazirene **12** is endothermic by 15−25 kcal/mol, an amount of energy that is readily available under both photolysis and thermolysis conditions. Although the 1*H*-diazirene rings in **12** and **13** are formally antiaromatic, **13** is a potentially observable species. The cyclic nitrile imine,[8,10,12] that is, the zwitterionic cumulene **17**, was also not observed. This molecule has a calculated energy 34 kcal/mol above that of the triplet nitrene and the strongest IR stretching vibration at 1538 cm^{-1}. There was no evidence for the formation of this compound, although reversible formation of **12**, **13**, **14**, **15**, **16**, **17**, and **18** cannot be ruled out (Scheme 1).

The observation of only a trace of triazacycloheptatetraene **14** (1990 cm^{-1} in the IR; see Figure S10) of course makes the identification of this molecule very tenuous, but strong evidence for the formation of the phenyl derivative **29** (2006 cm^{-1}) adds credence to the involvement of **14**. The ring opening to diradical **19** may take place from the seven-membered ring **14** and/or directly from the nitrene **11**. The calculated activation barrier for **14** → **19aOSS** (**TS5**, Scheme 2) is 18.9 kcal/mol at the CASSCF(8,8) level and 21.1 kcal/mol at the CASPT2 level (Table 1). On the triplet energy surface, the calculated barrier for **11T** → **19aT** (**TS3**, Scheme 2) is 28.8 kcal/mol (UB3LYP/6-31G*, Table 1). These calculations further indicate that the ring opening of **11T** to diradical **19aT** has a lower activation barrier than the formation of triazacycloheptatetraene **14** from diazirene **12** (28.8 vs 37.4 kcal/mol). Thus, the direct formation of diradical **19T** from **11** may be one of the most favorable reactions, keeping in mind that the calculations pertain to the ground states, whereas the photochemistry may take place on

(19) Casida, M. E. In *Recent Advances in Density Functional Methods*; Chong, D. P., Ed.; World Scientific: Singapore, 1995; Part I, p 155.
(20) Stratmann, R. E.; Scuseria, G. E.; Frisch, M. J. *J. Chem. Phys.* **1998**, *109*, 8218.
(21) NBO Version 3.1: Glendening, E. D.; Reed, A. E.; Carpenter, J. E.; Weinhold, F. Gaussian 03, revision C.01.
(22) Wasserman, E.; Snyder, L. C.; Yager, W. A. *J. Chem. Phys.* **1964**, *41*, 1763−1772.
(23) Tsao, M.-L.; Platz, M. S. *J. Phys. Chem. A* **2004**, *108*, 1169.

excited-state energy surfaces. Thus, there are two likely routes to **19**: type II ring opening of either nitrene **11** or triazacycloheptatetraene **14** via **TS3** and **TS5** (Scheme 2). Moreover, **14** may revert to **11**. The open-shell singlet nitrene **11OSS** lies only 7 kcal/mol above **14** by CASPT2, and the triplet **11T** lies 11−14 kcal/mol below. In the case of the phenyl analogue (Scheme 3), the triazacycloheptatetraene **29** is easily observable by IR spectroscopy, and reversion to the nitrene **27** on photolysis of the interconverting **29**/**33** mixture was observed by ESR spectroscopy.

The diradical **19** is of crucial importance, as it explains the formation of the products **21** and **22**. The formation of **21** as the first product (derived from the diradical **19b**) in the low-temperature matrix may be due to the fact that more motion is required for the formation of conformer **19c**, which has the correct orientation for the 1,4-H shift that leads to *anti*-**22**. The latter compound is stabilized in this conformation by a H-bond between NH and CN (2.7 Å long); thus, the energy of *anti*-**22** is calculated to be 6.5 kcal/mol below that of *syn*-**22**. The fact that the isomeric *o*-cyanophenylcarbodiimide (*o*-NC−C_6H_4−N═C═NH) was not detected indicates that *syn*-**22** is formed directly in this form and thus lends support to its genesis from diradical **19c**. The carbodiimide has almost the same calculated energy as *syn*-**22** (−36.4 kcal/mol). We do observe monosubstituted carbodiimides in other matrix reactions, when they are formed directly by different 1,7-H shifts, e.g., in the ylides analogous to **2** formed in type I ring opening reactions of 4-pyrimidylnitrene, 2-pyrazinylnitrene, 4-quinazolylnitrene, and 2-quinoxalinylnitrene.[10a,24] The reactions leading to **21** and **22** are highly exothermic (**21**, −26.4 kcal/mol; *anti*-**22**, −36.2 kcal/mol; relative to the energy of triplet nitrene **11**).

The photolysis of the phenyl derivative **25** demonstrates that the seven-membered ring **29** can indeed be obtained in good yield. Its longevity in this system could be due to the fact that a H has been replaced by Ph, so that the putative diradical **30** (Scheme 3) can no longer undergo a H shift, and a Ph shift to the anthranilonitrile **32** does not take place. This allows **29** to accumulate, although it is photochemically unstable under the conditions of its formation (>308 nm), where it is converted to diazo compound **33**. This reaction was not seen in Scheme 2, presumably because the ring opening reactions **11T** → **19T** and/or **14** → **19OSS** → **21** + **22** took preference. Importantly, the yield of cyanoindazole **31** also increases when **29** is bleached, which is a strong indication that at least some of **31** is formed from the seven-membered ring **29** (directly or via the diradical **30**).

Diazo compounds are 1,3-dipoles, of the same family as nitrile ylides and nitrile imines. Thus, the dipole-type ring opening of nitrene **27** and/or seven-membered ring **29** to diazo compound **33** is an example of type I ring opening as described in the Introduction.[3] The diradical-type ring openings to **19** and **30** are examples of type II ring opening.[3]

The matrix photolyses of both **9**/**10** and **25**/**26** also give rise to a third, minor, triplet species observable near 6900 G in the ESR spectra. **15**, **18**, and the phenylnitrene derivative (*Z*)-**20** are possible candidates for the minor nitrene species derived from **9**/**10**. In the case of the phenyl derivative **25**/**26**, the analogous minor nitrene is likely to be **34** (Scheme 3). These ring openings, **11T** → *Z*-**20T** and **27T** → *Z*-**34T**, have calculated activation barriers of ca. 34 and 35 kcal/mol, respectively (Table 1). They, too, are type II ring openings.

(24) Addicott, C.; Wong, M. W.; Wentrup, C. *J. Org. Chem.* **2002**, *67*, 8538−8546.

Conclusion

Argon matrix photolysis of tetrazolo[1,5-*a*]quinazoline/2-azidoquinazoline (**9**/**10**) affords **11**, observable by ESR, UV, and IR spectroscopy. A minor amount of a second nitrene formed by rearrangement to **18** or **15** or ring opening to the arylnitrene (*Z*)- **20** is also formed. The diradical **19** is formed by type II ring opening; it is detected by ESR spectroscopy but is thermally unstable, even at 15 K, where it decays with a half-life of ca. 47 min. Calculations indicate that this is due to its facile cyclization/rearrangement to the end products **21** and **22**.

Matrix photolysis of the 3-phenyl derivative **25** gives rise to the triazacycloheptatetraene **29**, which can be photochemically interconverted with the type I ring opening product 2-isocyano-α-diazo-α-phenyltoluene (**33**). Both **29** and **33** are characterized by Ar matrix IR spectroscopy. 4-Phenyl-2-quinazolinylnitrene (**27**) is observable by Ar matrix ESR spectroscopy. A second, minor, nitrene signal also observed in the ESR spectrum is likely to be due to ring opening to arylnitrene **34**. FVT of **9**/**10** and **25**/**26** affords the ring contraction products **21** and **31**, respectively, as the main products.

Experimental Section

The apparatus and procedures for preparative FVT[25] and for Ar matrix isolation[26] were as previously described. The internal oven employed a 10 cm long, 0.7 cm i.d., electrically heated quartz tube suspended in a vacuum chamber directly flanged to the cryostat cold head, with a wall-free flight path of ca. 3 cm between the exit of the quartz tube and the cold target (KBr or CsI for IR spectroscopy, quartz for UV spectroscopy, and a Cu rod (7 cm long, 1.5 mm i.d.) for ESR spectroscopy). The external oven consisted of a 20 cm (0.7 cm i.d.) quartz tube ending in a quartz flange directly flanged to the cryostat cold head; this tube was heated on a 10 cm length and had a ca. 5 cm unheated length connecting it to the cold head. FVT products were isolated in liquid nitrogen (77 K) in the preparative thermolyses, at 7−22 K with Ar for matrix isolation IR and UV experiments and at 15 K with Ar for ESR experiments. Photolysis experiments used a 1000 W high-pressure Xe/Hg lamp equipped with a monochromator and appropriate filters, a 75 W low-pressure Hg lamp (254 nm), and excimer lamps operating at 222 nm (25 mW/cm^2) and 308 nm (50 mW/cm^2). IR spectra were recorded with a resolution of 1 cm^{-1}. ESR spectra were recorded on an X-band spectrometer. GC for GC−MS analysis was performed on a 30 m capillary column, injector port temperature 200 °C, temperature program 100 °C for 2 min and then 16 °C/min till 270 °C. Melting points are uncorrected.

N-Cyanoanthranilonitrile (**22**),[11b] 6-phenyltetrazolo[1,5-*a*]quinazoline (**25**),[27] and 3-phenylindazole[28] were prepared according to literature methods.

Tetrazolo[1,5-*a*]quinazoline (9). 2-Chloroquinazoline (1.50 g; 9.1 mmol) and sodium azide (1.17 g; 18 mmol) were dissolved in 7.5 mL of 0.5 M HCl containing 10% EtOH. The mixture was refluxed for 2 h, cooled to room temperature, and filtered, and the resulting crystalline product was purified by column chromatography on silica gel, eluting with $CHCl_3$−MeOH (99:1) to yield 866 mg (55%) of **9** as a white solid: mp 224−226 °C; ^{1}H NMR ($CDCl_3$)

(25) Wentrup, C.; Blanch, R.; Briehl, H.; Gross, G. *J. Am. Chem. Soc.* **1988**, *110*, 1874.
(26) Kuhn, A.; Plg, C.; Wentrup, C. *J. Am. Chem. Soc.* **2000**, *122*, 1945. Kappe, C. O.; Wong, M. W.; Wentrup, C. *J. Org. Chem.* **1995**, *60*, 1686.
(27) Bogatskii, A. V.; Andronati, S. A.; Zhilina, Z. I.; Danilina, N. I. *Zh. Org. Khim.* **1977**, *13*, 1773−1780.
(28) Borsche, W.; Scriba, W. *Justus Liebigs Ann. Chem.* **1939**, *540*, 83.

δ 9.38 (s, 1 H), 8.65 (d, J = 8 Hz, 1 H), 8.21 (d, J = 8 Hz, 1 H), 8.15 (t, J = 8 Hz, 1 H), 7.87 (t, J = 8 Hz, 1 H); ^{1}H NMR ($CDCl_3$-CF_3COOH (1:1)) (minor isomer **10**) δ 9.77 (s, 1 H), 8.80 (d, 1 H), 8.50 (d, 1 H), 8.40 (t, 1 H), 8.10 (t, 1 H); (major isomer **9**) δ 9.73 (s, 1 H), 8.35 (d, 1 H), 8.30, (t, 1 H), 8.05 (d, 1 H), 7.95 (t, 1 H); ratio **10**:**9** = 21:79; ^{13}C NMR ($CDCl_3$) δ 160.8 (CH), 151.6 (C quart), 136.2 (CH), 130.9 (C quart), 129.3 (CH), 128.9 (CH), 117.8 (C quart), 114.1 (CH) ppm; the assignments are supported by a DEPT-135 spectrum. The Ar matrix IR spectrum is shown in Figure S1. Anal. Calcd for $C_8H_5N_5$: C, 56.14; H, 2.94; N, 40.92. Found: C, 55.99; H, 2.79; N, 40.86.

Matrix Isolation of Azide 10. 9 (ca. 10 mg) was sublimed at 105 °C through an external quartz oven (200−230 °C for photolysis experiments, 430−600 °C for FVT) under vacuum (2.0×10^{-6} mbar) and codeposited with Ar (5 mbar/min from a 2 L reservoir filled with 1 atm of Ar). The Ar matrix IR spectrum is shown in Figure S2.

Matrix Photolysis of Tetrazolo[1,5-*a*]quinazoline/2-Azidoquinazoline (9/10). The matrix photolysis of tetrazole **9**/azide **10** yielded 1-cyanoindazole (**21**) and *N*-cyanoanthranilonitrile (**22**). A brief photolysis of **10** (Ar, 10 K, 308 nm, 30 s) afforded species **21** absorbing at 2260 cm^{-1}. In the course of further photolysis another new species rapidly grew in at 2255 cm^{-1}, and this was the main species after long photolysis times (25 h) with 254 nm. Complete conversion of azide to **22** was not possible even after 2 days of photolysis with 308, 254, and 222 nm. Bands due to **22** are at 3411, 3406 w, 2255 w (NHCN), 2236 vw (CN), 1595 m, 1511 m, 1439 w, 1306 w, 1256 vw, 1167 vw, and 757 m cm^{-1}.

1-Cyanoindazole (21). Sodium hydride (90 mg, 3.75 mmol) was added to a solution of 413 mg (3.5 mmol) of indazole in 30 mL of toluene, and the mixture was stirred for 1 h. Cyanogen bromide (556 mg, 5.2 mmol) in 10 mL of toluene was added dropwise, and the resulting mixture was refluxed for 3 h. After filtration and removal of the solvent and excess BrCN in vacuo, the resulting product was sublimed at 55−60 °C (10^{-2} mbar) to afford 300 mg (60%) of **21**: mp 70−72 °C; ^{1}H NMR ($CDCl_3$) δ 8.23 (s, 1 H), 7.80 (d, 1 H, J = 8 Hz), 7.67 (t, 1 H, J = 7 Hz), 7.64 (t, 1 H, J = 8 Hz), 7.41 (t, 1 H, J = 7 Hz); MS m/z = 143. The Ar matrix IR spectrum is shown in Figure S11. Anal. Calcd for $C_8H_5N_3$: C, 67.13; H, 3.50; N, 29.37. Found: C, 67.03; H, 3.43; N, 29.41.

21 by Preparative FVT of Azide 9. Tetrazole **9** (100 mg) was subjected to preparative FVT at 600 °C. The product was isolated in a liquid N_2 trap and purified by column chromatography on silica gel and sublimation at 55−60 °C (10^{-2} mbar) to afford **21** (62%), mp 70−72 °C, with properties identical with those described above.

Matrix Isolation of 21. Tetrazole **9**/azide **10** was sublimed into the FVT tube in a stream of Ar at 106−108 °C and thermolyzed at 500 °C. The products were isolated in an Ar matrix at 20 K, and FTIR spectra were recorded at ca. 10 K. A typical IR spectrum of the thermolysis product **21**, and the calculated spectrum, together with the spectrum of authentic material, is shown in Figure S11. Bands due to **21** (Ar, 10 K) are at 2260 s (CN), 1618 vw, 1507 w, 1429 m, 1373 w, 1149 vw, 1027 w, 908 w, 748 m, and 746 m cm^{-1}.

Semipreparative FVT of Azide 9. Experimental conditions for the FVT of **9** and matrix isolation of the products were as described above. After the ESR experiments, the copper rod was rinsed with dichloromethane (2 mL) and the products were analyzed by GC−MS to give the following composition: tetrazole **9** (60% at 430 °C, 0% at 600 °C, R_t = 9.43 min, m/z = 171), 2-aminoquinazoline (**23**) (11% at 430 °C, 35% at 600 °C, R_t = 7.36 min, m/z = 145), **21** (28% at 430 °C, 65% at 600 °C, R_t = 5.96 min, m/z = 143), and indazole (**24**) (0.6% at 430 °C, 1.8% at 600 °C, R_t = 5.66 min, m/z = 118), all identified by comparison with the authentic materials.

1-Cyano-3-phenylindazole (31). Tetrazole **25**/azide **26** (mp 202−203 °C; 0.45 g, 1.82 mmol) was subjected to preparative FVT at 380 °C in the course of 4 h. The resulting product was sublimed at 65−75 °C/10^{-3} mbar to afford 0.25 g (63%) of white, slightly lachrymatory crystals of **31**; mp 95−96 °C; very soluble in ether; MS m/z 219; IR (KBr) 2255, 1640 cm^{-1}; IR (Ar, 10 K) 2256 vs, 1617 w, 1495 m, 1365 s, 1357 m, 1150 w, 1111 w, 1064 m, 783 m, 769 w, 745 m, 697 m, 579 w cm^{-1}. Anal. Calcd for $C_{14}H_9N_3$: C, 76.70; H, 4.11; N, 19.18. Found: C, 76.64; H, 4.22; N, 19.22.

A 0.02 g portion of **31** was hydrolyzed with 5 mL of 0.2 N NaOH at 125 °C for 3 h. After the solution was cooled to room temperature, the precipitate was filtered off, and the solution was neutralized and extracted with EtOAc. The extract was evaporated to dryness, and the resulting solid was recrystallized from petroleum ether or sublimed at 100 °C/10^{-2} mbar to afford 3-phenylindazole: mp 114−116 °C (lit.[26] mp 115−116 °C).

Matrix Isolation of Azide 26. Tetrazole **25** was sublimed at 150 °C, and the vapor was passed through the FVT tube at 200 °C and then deposited with Ar at 22 K. IR (Ar, 10 K): 2174 w, 2137 s, 2131 s, 2109 w, 1620 m, 1569 m−s, 1552 s, 1543 s, 1327 vs, 1265 m, 1233 m, 777 w, 699 m, 636 w cm^{-1}.

Acknowledgment. This work was supported by the Australian Research Council, the APAC national supercomputing facility (merit allocation scheme), and the Centre for Computational Molecular Science at The University of Queensland. We thank Dr. Michael Kiselewski for preliminary experiments and calculations, Mr. Riko Burgard for assistance with some experiments, and Dr. Tri Le and Mr. George Spatny for untiring help keeping the ESR spectrometer running.

Supporting Information Available: Experimental and calculated IR spectra, $D-\rho$ correlation for over 100 nitrenes, ESR spectra of nitrenes, diradicals, and carbene **37**, kinetics of decay of triplet diradical at 15 K, UV−vis spectrum of **33**, Cartesian coordinates, absolute energies, and frequencies or electronic transitions of compounds calculated at the B3LYP/6-31G**, B3LYP/6-31G*, TDB3LYP/6-31G**, and CASSCF(8,8)/6-31G* or CASPT2 levels, and structures and spin densities of triplet nitrenes and diradicals **19a**−**c** (UB3LYP/EPRIII). This material is available free of charge via the Internet at http://pubs.acs.org.

JO052541I